Theoretical Investigation of the Binding Energies of the Iodide Ion and Xenon Atom with Decaborane

Ilias Sioutis and Russell M. Pitzer*

Department of Chemistry, The Ohio State University, 100 W. 18th Ave., Columbus, Ohio 43210

Received: July 13, 2006; In Final Form: August 28, 2006

The interaction of decaborane ($B_{10}H_{14}$) with the I^- ion and the (isoelectronic) Xe atom is investigated using a number of theoretical methods: MP2, CCSD(T), CCSD, spin−orbit CISD, and DFT using the B3LYP, B3PW91, PW91PW91, and PBE0 methods. All non-DFT and some DFT methods agree that $B_{10}H_{14}I^-$ is bound by charge−dipole electrostatic forces, charge− and dipole−induced-dipole forces, and dispersion forces, while $B_{10}H_{14}Xe$ is bound by dipole−induced-dipole forces and dispersion forces. Counterpoise corrections are necessary to obtain reliable results. Relativistic effective core potentials were used for the I, Xe, and B atoms. Basis sets for use with these potentials are discussed as is the question of basis set balance in molecules. We find $B_{10}H_{14}I^-$ to be bound by 19.8 kcal/mol and $B_{10}H_{14}Xe$ by 1.1 kcal/mol, indicating that the charge and polarizability of I^- play the major role in the interaction energy.

1. Introduction

Decaborane ($B_{10}H_{14}$) exhibits a wide range of properties, the investigation of which has previously[1] led to the preparation for the first time of an interesting complex ion formed between the iodide ion and decaborane, namely, $B_{10}H_{14}I^-$ (see Figure 1).

Under certain experimental conditions, $B_{10}H_{14}I^-$ is found to be stable both in the solid state and in solution.[1] The X-ray crystal structure of 2,4-$I_2B_{10}H_{12}I^-$ (in Figure 1 but with hydrogen atoms attached to B(10) and B(9) instead of iodine atoms) reveals C_{2v} symmetry.[1] The formation of the $B_{10}H_{14}I^-$ complex results in some perturbation of the $B_{10}H_{14}$ framework, as is experimentally evident from the ^{11}B and ^1H NMR, Raman, IR, and visible spectra.[1] The unique iodide is situated at the open end of the decaborane, effectively resting on the four bridging hydrogens. Iodide presumably transfers electronic charge to the lowest unoccupied molecular orbital (LUMO) of the electron-deficient $B_{10}H_{14}$ by interacting with the positive end of decaborane. While the bridging hydrogens are believed to act as Lewis acids, the boron atoms B(1) and B(2) become susceptible to nucleophilic attack.[1] However, the interaction involves distances which are consistent with van der Waals interactions. On the other hand, the polar nature of decaborane and the charge of the iodide ion suggest a charge−dipole electrostatic and charge− and dipole−induced-dipole contributions to the interaction energy of this molecular system.

The purpose of this work is to study the nature of this interaction and describe the electronic charge transfer from the iodide ion to $B_{10}H_{14}$. In doing so, we have computed the ground-state interaction energy of the iodide ion with decaborane in the complex $B_{10}H_{14}I^-$. Our principal results reveal the most important term in the interaction energy of $B_{10}H_{14}I^-$ to be electrostatic. We have also focused our attention on $B_{10}H_{14}Xe$, an unknown compound isoelectronic to $B_{10}H_{14}I^-$. We have determined the ground-state interaction energy of $B_{10}H_{14}Xe$ and compared the electronic structure characteristics of it with $B_{10}H_{14}I^-$. We find $B_{10}H_{14}Xe$ to be weakly bound by dispersion forces.

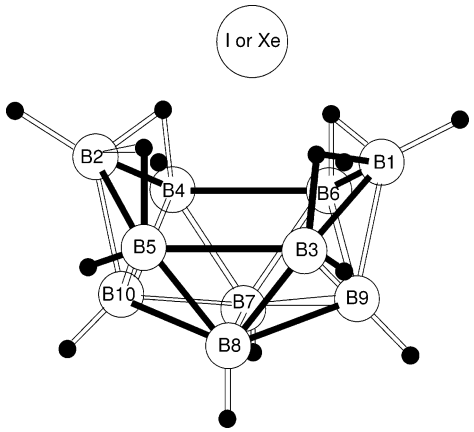

Figure 1. The molecular configuration and numbering scheme of $B_{10}H_{14}I^-$ and $B_{10}H_{14}Xe$. The bridging hydrogens (μ−H) are between B(2), B(4,5) and B(1), B(6,3). There is no bond between B(4), B(5) and B(6), B(3), but between B(4), B(5), and B(10), and B(6), B(3), and B(9).

The calculation of an accurate molecular binding energy involves the use of an accurate correlation treatment and adequate basis sets. The wave function based methods that we apply are restricted Hartree−Fock self-consistent-field theory (SCF), (single-reference) spin−orbit single- and double-excitation configuration interaction (SO−CISD), using configuration state functions (CSFs) with spin quantum numbers 0, 1, and 2, second-order Møller−Plesset perturbation theory (MP2), coupled-cluster theory with single and double excitations (CCSD), and CCSD(T), which also includes perturbation-theory values of the connected-triple-excitation terms. We also compare these results with density functional theory (DFT) calculations with four different exchange-correlation functionals.

2. Theoretical and Computational Methods

2.1. Evaluation of the Interaction Energy. The method used to evaluate the interaction energy between two interacting systems (suitable for either weak or strong binding) is based

10.1021/jp064437q CCC: $33.50
Published on Web 10/25/2006

on the supermolecular approach, which is an important choice for non-size-extensive methods.

Basis set superposition error (BSSE) in the evaluation of the interaction energy[2] is a matching or balancing error.[3] We apply the function counterpoise procedure (CP)[4] as a way to correct for it.

While simple implementation of BSSE is suitable for the evaluation of the interaction energy between two monomer units, further improvement of it may become necessary in the case that the monomers are molecules. In principle, the energy change for distorting the monomers from their isolated geometries to the ones in the complex (known as fragment relaxation energy or deformation energy[5,6]) should also be included. However, as a first approximation, these terms were neglected in our evaluation of the interaction energy between $B_{10}H_{14}$ and I^- ion and Xe.

2.2. Core Potentials. We use the relativistic effective core potential (RECP) approximation in order to properly describe the relativistic effects of the many-electron systems that we study and, in particular, the RECPs developed by Christiansen et al.[7−12] These potentials replace inner-shell (core) electrons and orbitals by a repulsive potential. These RECP techniques[13,14] describe the valence space in terms of pseudo-orbitals which are identical to the corresponding all-electron valence orbitals in the valence region, but go smoothly to zero in the core region. The RECP methodology is advantageous for our work because (i) more electrons can be removed from the computation, (ii) relativistic corrections are easily incorporated into RECPs, and (iii) it is possible to obtain one-electron spin−orbit operators simultaneously with the RECPs, at the same level of approximation.

With the core electrons removed from the problem, the Hamiltonian includes the nonrelativistic Hamiltonian for the valence electrons (kinetic energy and Coulomb terms) plus the RECPs and spin−orbit operators. The spin−orbit operators include the (large) spin−orbit interactions of the valence electrons with the nucleus and with the core electrons as well as an approximation[15] to the (small) spin−orbit interaction between the valence electrons. The boron core[7,8] is the 1s shell (2 electrons), and both the iodine and xenon cores are the 1s through 4p shells (36 electrons). Thus, in $B_{10}H_{14}I^-$ and $B_{10}H_{14}Xe$, 56 electrons (core) were removed from the calculations and 62 electrons (valence) were treated explicitly.

2.3. Basis Sets. Most atomic-orbital (AO) basis sets available for use with RECPs are those originally published with the RECPs. The basis sets we use in this work, however, include more recent improvements as described below. A common method of choosing contractions for basis sets is to use occupied atomic SCF orbitals for the basic contractions and then free up some number of the more diffuse primitive functions for additional contractions.[16] However, the RECP methodology requires the valence pseudo-orbitals to have a small amplitude in the core region and go smoothly and nodelessly to zero at the nucleus.[14,17,18] Correspondingly, suitable additional contractions have been chosen to satisfy these properties. This is most commonly known as the one-center effect[17] and can be addressed in several ways.[17,18] Christiansen uses an augmentation scheme[17] that involves the formation of two-primitive contractions with coefficients that give exact cancellation of the leading power of r at the origin. He finds that augmented (aug. in the tables) primitives are unnecessary for d and higher angular momentum orbitals.

However, orbitals centered on a neighboring atom B may have moderate magnitude in the core region of atom A. This problem, known as the two-center effect,[17] requires further change in the A basis set. Christiansen adds an additional s contraction to the basis set on atom A such that the next-most-diffuse primitive function is freed. This s contraction has a large amplitude in the core region so that, in the formation of the molecular orbitals (MOs), it can be used to cancel out the amplitudes of the B orbitals in the A core region. This s contraction will also lead to a virtual MO which has such high energy it will not contribute significantly to correlation energy calculations and hence may be omitted from them. This additional s contraction makes it unnecessary to use augmented s functions.

TABLE 1: I cc-pVTZ Basis Set: (5s5p5d1f)/[4s3p3d1f]

orbital	primitives	contraction	contraction	contraction	contraction
s	3.072	0.048359	0.0	0.0	0.0
	0.9631	−0.806443	0.0	0.0	0.0
	0.5303	0.674366	0.0	0.0	1.0
	0.2070	0.683570	1.0	0.0	0.0
	0.09835	0.242690	0.0	1.0	0.0
p	9.624	−0.002450	0.0	0.0	
	0.9464	−0.218667	0.0	0.0	
	0.4591	0.458951	−0.298228	0.0	
	0.1744	0.582505	1.0	−0.310319	
	0.06839	0.208211	0.0	1.0	
d	31.53	−0.012148	0.0	0.0	
	4.724	0.203370	0.0	0.0	
	2.399	0.470191	0.0	0.0	
	1.100	0.378001	1.0	0.0	
	0.4419	0.101520	0.0	1.0	
f	0.701216	1.0			

We used the iodine basis set shown in Table 1, which, except for the f polarization function, was developed by Christiansen in a correlation-consistent (cc) manner[16,19] and has polarized triple-ζ (cc-pVTZ) quality. The resulting basis set is of (5s5p5d1f)/[4s3p3d1f] size, where this notation represents (primitives)/[contractions]. It includes freed-up diffuse primitives for s, p, and d (augmented for p). We refer to this basis set in the tables as "diffuse + tight s + aug. p + f(0.701266)". We also wanted to find out how much valence correlation energy can be recovered using Christiansen's contraction methods. Our results are tabulated in Table 2. In the same table, we include the SCF and CISD energies that result from inclusion of an f polarization function. Both choices of exponent for the f function came from cc valence basis sets for use with the Stuttgart−Dresden−Bonn (SDB) (46-electron core) RECPs.[20,21] Similar values are available from basis sets for 28-electron RECPs.[22]

Our xenon basis set is a cc polarized double-ζ (cc-pVDZ) set and is shown in Table 3. The primitive functions are those provided with the RECP.[10] We freed up the two most diffuse s primitives and the most diffuse p (augmented) primitive, as well as adding one more d function (exponent 0.22865) to polarize the 5p shell since none of the primitives for the 4d shell were diffuse enough to serve this purpose. The two most diffuse d primitives were left uncontracted. We then performed CISD calculations using a series of f polarization functions[20,21] and found that an exponent of 0.801144 was best. The contractions were chosen in a way that would make the basis set similar to a cc-pVDZ basis set. Its size is (3s3p5d1f)/[3s2p3d1f].

We have developed our own RECP basis set for boron,[19] as shown in Table 4. It is of cc-pVDZ size, (4s4p1d)/[3s2p1d]. The hydrogen basis set[23] is also of cc-pVDZ size, (4s1p)/[2s1p].

2.4. Computational Methods. For both the (closed-shell) ground electronic states of $B_{10}H_{14}I^-$ and $B_{10}H_{14}Xe$, the SCF and SO−CISD calculations were performed using the COLUM-

TABLE 2: SCF and SO−CISD Energies Relative to −144 E_h for $B_{10}H_{14}I^-$ at Its Equilibrium Geometry Using Various Basis Set Contraction Schemes on the I Atom[a]

primitives	E(SCF)	E(SO−CISD)	ΔE
diffuse	−0.642918	−1.578548	−0.935629
aug. s	−0.642823	−1.579481	−0.936658
diffuse + tight s	−0.642932	−1.581517	−0.938585
diffuse + tight s + aug. p	−0.643107	−1.600639	−0.957532
diffuse + tight s + aug. p + f(0.429319)	−0.643192	−1.638329	−0.995137
diffuse + tight s + aug. p + f(0.701216)[b]	−0.643158	−1.663509	−1.020351

[a] The ΔE values are correlation energies (in E_h). [b] Basis set in Table 1.

TABLE 3: Xe cc-pVDZ Basis Set: (3s3p5d1f)/[3s2p3d1f]

orbital	primitives	contraction	contraction	contraction
s	0.7127	−2.536570	0.0	0.0
	0.5719	2.742737	1.0	0.0
	0.1519	0.638936	0.0	1.0
p	1.2353	−0.141311	0.0	
	0.3726	0.644602	−0.249969	
	0.1229	0.511983	1.0	
d	4.5119	0.266105	0.0	0.0
	2.4799	0.385422	0.0	0.0
	1.2983	0.365995	0.0	0.0
	0.5435	0.124862	1.0	0.0
	0.22865	0.0	0.0	1.0
f	0.801144	1.0		

TABLE 4: B cc-pVDZ Basis Set: (4s4p1d)/[3s2p1d]

orbital	primitives	contraction	contraction	contraction
s	14.55	−0.0103380	0.0	0.0
	2.259	−0.1368565	0.0	0.0
	0.3076	0.5752983	0.0	1.0
	0.09889	0.5324867	1.0	0.0
p	5.984	0.0355794	0.0	
	1.239	0.1982340	0.0	
	0.3358	0.5058596	0.0	
	0.09527	0.4785609	1.0	
d	0.3477	1.0		

BUS system of quantum chemistry programs.[24] The SO−CISD method is implemented in COLUMBUS in combination with RECPs and spin−orbit operators.

The binding energies of $B_{10}H_{14}I^-$ and $B_{10}H_{14}Xe$ were computed at additional levels of theory with the *NWChem*[25] computational chemistry package. The wave function based methods include MP2, CCSD,[26−28] and CCSD(T).[29,30] We performed DFT calculations within the Kohn−Sham[31,32] formalism. Several functionals were used: the Becke three-parameter exchange functional with the Lee−Yang−Parr correlation functional (B3LYP),[33,34] the same exchange functional with the Perdew−Wang91 (PW91) correlation functional (B3PW91),[33,35] PW91 for both exchange and correlation (PW91PW91),[35] and the functional PBE0.[36]

In all cases, we used the same basis sets and RECPs. Some of these calculations included the spin−orbit interaction. These were SO−CISD and some separate DFT calculations (SO−DFT) for the cases that the DFT functional gave binding energies close to our CCSD(T) results (most accurate correlation treatment). The SO−DFT results were used merely as an indication of the contribution of the spin−orbit interaction to the binding energy in DFT theory. We also note that, for the wave function based calculations, we included all occupied and virtual MOs.

For $B_{10}H_{14}Xe$, our initial effort focused on the optimization of the intermolecular distance R between $B_{10}H_{14}$ and Xe at the SO−CISD level of theory. We kept the $B_{10}H_{14}$ atoms fixed at the crystallographic geometry. The position of the minimum (R_e) of the potential surface of $B_{10}H_{14}Xe$ was obtained by fitting parabolas to three points.

TABLE 5: SCF and Spin−Orbit CI (singles and doubles) Energies (in E_h) for $B_{10}H_{14}I^-$ at R_e and at $R = 100$ (both in b)[a]

	SCF	SO−CISD
$R_e = 7.18183$	−144.643158	−145.663509
$R = 100$	−144.621418	−145.632860
ΔE	13.64	19.23

[a] ΔE is the dissociation energy (in kcal/mol).

TABLE 6: Ground-State $B_{10}H_{14}$ SCF Mulliken Population Analysis[a]

	gross atomic populations								
atom	B(2)	B(4)	B(8)	B(10)	H(2)	μ−H	H(4)	H(10)	H(8)
total	2.916	3.061	3.007	3.021	0.985	0.967	0.998	1.017	1.001

[a] Boron has three valence electrons, and the labels refer to the symmetry-distinct atoms. The labels of the hydrogens are the same as those of the borons that they are bonded to, and μ−H is for the bridging hydrogens.

3. Results

3.1. Ground-State SCF Results for $B_{10}H_{14}I^-$. The ground-state SCF energy of $B_{10}H_{14}I^-$ was computed at $R_e = 7.18183$ b between the center of mass of the atoms B(4,6,3,5) of $B_{10}H_{14}$ and I^- determined from the X-ray analysis (Table 5 and Figure 1). We also made an SCF calculation at an interfragment distance of 100 b, since the supermolecule is composed of two noninteracting closed-shell subsystems.

The dissociation products are well-represented by closed-shell wave functions, so closed-shell SCF calculations give the correct size-consistent behavior in the limit of large intermolecular distance. Of particular interest is the comparison of the occupied MO spectrum that is obtained at a situation of no molecular interaction with that at the equilibrium geometry.

The highest occupied MOs are I 5p/5s orbitals (symmetries A_1, B_1, B_2, A_1) at $R = 100$ b, but they show mixing with other AOs at the equilibrium geometry of $B_{10}H_{14}I^-$, particularly with AOs centered on all the B atoms and on the bridging hydrogens (see Figure 1). The orbital energies (E_h) of these MOs are −0.167 (A_1), −0.164 (B_1), −0.163 (B_2), and −0.652(A_1). The partial gross atomic populations for these occupied MOs suggest electron charge transfer of ca. 0.1 electron from the iodide to the B atoms. The most important charge transfer takes place from the A_1 5p iodide orbital. The lowest unoccupied MO of $B_{10}H_{14}$ (orbital energy 0.047 and A_1 symmetry) consists of orbitals mostly centered on the same atoms to which charge transfer has been noted.

Decaborane is a polar molecule with positive character at the open face of the B4 basket. The population analysis of $B_{10}H_{14}$ is given in Table 6. The bridging hydrogens and B(2,1) atoms (Figure 1) are electron deficient, and are therefore Lewis

TABLE 7: Ground-State $B_{10}H_{14}I^-$ SCF Mulliken Population Analysis[a]

	gross atomic populations									
atom	B(2)	B(4)	B(8)	B(10)	H(2)	μ−H	H(4)	H(10)	H(8)	I(1)
total	2.921	3.067	3.034	3.075	0.992	0.916	1.014	1.027	1.007	17.896

[a] The number of valence electrons is 3 for boron and 18 for iodide. The labels refer to the symmetry-distinct atoms. The labels of the hydrogens are the same as those of the borons that they are bonded to, and μ−H is for the bridging hydrogens.

acids, and the B(2) and B(1) sites are susceptible to nucleophilic attack. A comparison of the gross atomic populations between $B_{10}H_{14}$ and $B_{10}H_{14}I^-$ is a useful indication for the transfer of electronic charge. Table 7 shows the population analysis of $B_{10}H_{14}I^-$. The magnitude of the charge transfer from iodide is apparent and somewhat surprising in that the bridging hydrogens become more electron deficient upon the formation of $B_{10}H_{14}I^-$. The electron charge transferred is distributed among all remaining atoms of the molecule with emphasis on those of B(10,9) and B(7,8).

Our SCF results are in agreement with the experimental results.[1] We find that B(2) and B(1) of $B_{10}H_{14}$ are susceptible to nucleophilic attack even upon formation of $B_{10}H_{14}I^-$, and this finding is in agreement with experimental results.[1,37,38] While population analyses are known to be particularly sensitive to basis set choice, especially when diffuse basis functions are involved, one may still assign physical significance to such results as long as the basis sets are balanced. Although the iodine basis set is larger than those of boron and of hydrogen, care has been taken that the number of basis functions describing the valence space of iodide is proportional to the number of valence electrons. In an analogous way, the same proportionality is kept, approximately, for boron and hydrogen. In this way, we try to keep a proper balance among the basis sets of the system. The alternative of using pVDZ basis sets for both B and I would probably lead to less balanced results.

3.2. Single-Reference SO−CISD Results for $B_{10}H_{14}I^-$. We performed single-reference SO−CISD calculations for the ground state of $B_{10}H_{14}I^-$, using the SCF MOs and including excitations from all occupied MOs to all unoccupied MOs, generating a total of 4.3×10^7 CSFs. The reference configuration of $B_{10}H_{14}I^-$ at the equilibrium geometry has a CI coefficient close to 0.88. Three of the four highest contributing doubly excited configurations are also basic doubly excited configurations for the CI expansion of decaborane with almost the same CI coefficients as those in the CI expansion of $B_{10}H_{14}I^-$ at its equilibrium geometry. We examined the SCF MOs from which the electrons are excited along with the MOs that the electrons go into. The excitations go from the $6b_1$ and $7b_2$ occupied MOs to the lowest-energy virtual MOs of A_1 symmetry and A_2 symmetry. The principal coefficients for $6b_1$ come from the 2p orbitals on the B(10) group of atoms and also those on the B(4) group of atoms. The $7b_2$ MO has significant mixing of the 2p orbitals from the B(10), B(8), and B(2) groups of atoms. The lowest virtual of A_1 symmetry has its principal coefficients from the 2p and 2s orbitals on the B(4) and B(2) group of atoms, and the lowest virtual MO of A_2 symmetry has its principal coefficients from the 2s and 2p orbitals on the B(4,6,3,5) group of atoms. The fourth excited configuration has excitation from $7b_1$ to an A_1 symmetry virtual MO and from $8b_2$ to an A_2 symmetry virtual MO. The $7b_1$ and $8b_2$ MOs are the highest-energy occupied MOs and have iodide 5p character. The principal coefficients for the A_1 virtual MO are for 2s and 2p orbitals on the B(8) group of atoms and for 2s orbitals on the B(10) group of atoms. The A_2 virtual MO has principal coefficients from 1s orbitals on the bridging hydrogens and also from 2p orbitals on the B(4) group of atoms and from 4d orbitals on the iodide ion. At the supermolecular separation of 100 b, we notice the same doubly excited configurations of decaborane with almost the same CI coefficients and with excitations from the same types of occupied MOs to the same types of virtual orbitals. There are also a significant number of doubly excited configurations involving excitations from 5s, 5p, and 4d orbitals on iodide to higher-energy s and p MOs on iodide.

According to Table 5, the binding energy between decaborane and the iodide ion has been calculated as 19.23 kcal/mol at the SO−CISD level, which is 5.59 kcal/mol more than the corresponding SCF result. This additional contribution to the binding energy upon inclusion of correlation and spin−orbit effects for $B_{10}H_{14}I^-$ signifies their importance in this type of binding energy.

3.3. MP2, CCSD, CCSD(T), and DFT Results for $B_{10}H_{14}I^-$. Tables 10 and 11, respectively, contain the binding energies from all the theoretical methods, both without and with the CP corrections. In Table 10, we note the importance of the triple excitations as a correction to the CCSD approximation. The CCSD(T) results have the most accurate correlation treatment but do not include spin−orbit effects. However, the CCSD binding energy is close to the SO−CISD result already mentioned. Also, the MP2 result shows close agreement with

TABLE 8: SCF and Spin−Orbit CI (singles and doubles) Energies (in E_h) for $B_{10}H_{14}Xe$ at $R_e = 8.73293$ b and at $R = 100$ b[a]

	SCF	SO−CISD
$R = R_e$	−160.936594	−161.926417
$R = 100$	−160.936959	−161.924894
ΔE	−0.23	0.96

[a] ΔE denotes the dissociation energy (in kcal/mol).

TABLE 9: Ground-State $B_{10}H_{14}Xe$ SCF Mulliken Population Analysis at $R_e = 8.73293$ and $R = 100$ b[a]

	gross atomic populations									
R	B(2)	B(4)	B(8)	B(10)	H(2)	μ−H	H(4)	H(10)	H(8)	Xe
R_e	2.923	3.061	3.005	3.022	0.985	0.965	0.998	1.017	1.001	17.992
100	2.917	3.061	3.007	3.020	0.986	0.967	0.998	1.017	1.001	18

[a] The number of valence electrons is 3 for boron and 18 for xenon. The labels refer to the symmetry-distinct atoms. The labels of the hydrogens are the same as those of the borons that they are bonded to, and μ−H is for the bridging hydrogens.

TABLE 10: Wave Function Based Results for $B_{10}H_{14}I^-$ [a]

method	BE, ΔE^{CP}	BE, ΔE^{noCP}
CCSD(T)	19.84	25.30
CCSD	18.95	23.96
MP2	20.75	26.04
SO−CISD		19.23
SCF		13.64

[a] The binding energy (BE) is in kcal/mol and CP denotes counterpoise procedure.

TABLE 11: DFT and SO-DFT Results for $B_{10}H_{14}I^-$ [a]

functionals	BE, ΔE^{CP}	BE, ΔE^{noCP}
B3LYP	17.02	17.65
B3PW91	19.76	20.24
PW91PW91	21.68	22.47
PBE0	20.91	21.44
B3PW91(SO-DFT)	19.84	

[a] The binding energy (BE) is in kcal/mol and CP denotes counterpoise procedure.

the CCSD(T) calculations, so it provides a relatively good estimate of the binding energy. This has been seen previously; perturbation theory methods (even at a second-order level) provide an adequate description of weakly bonded systems whose binding is mostly electrostatic.[39] Table 11 shows that the B3LYP method underestimates the binding energy of $B_{10}H_{14}I^-$, while PW91PW91 and PBE0 for the CP-corrected binding energies show the opposite effect, a result owing possibly to fortuitous cancellations of inaccuracies in the exchange and correlation functionals being used. In contrast, B3PW91 gives a good estimate of the binding energy, slightly lower than our CCSD(T) results. Inclusion of the spin−orbit interaction makes a difference in the case of $B_{10}H_{14}I^-$, giving a result that turns out to be the same as our CCSD(T) results (which do not include the spin−orbit interaction).

3.4. Ground-State SCF Results for $B_{10}H_{14}Xe$. $B_{10}H_{14}Xe$ is also a closed-shell system that, at large distance ($R = 100$ b), separates into closed-shell subsystems. This makes the closed-shell SCF calculation applicable to the whole potential surface characterizing the separation of fragments, giving a convenient reference configuration for several correlation methods.

We compared the ground-state occupied MOs for $B_{10}H_{14}Xe$ at the equilibrium distance at $R_e = 8.73293$ b and at $R = 100$ b and noticed differences for energetically neighboring occupied MOs. The MO $10a_1$ (orbital energy -0.491 E_h) at R_e has Xe 5p as its largest coefficient. It has smaller coefficients on the 2p AOs of the B(2), B(4), B(8), and B(10) groups of atoms (see Figure 1) and 1s AOs of the bridging hydrogens, H(10) and H(8) atoms. However, at 100 b, this MO is entirely on the $B_{10}H_{14}$. The $11a_1$ (-0.475 E_h) is composed mostly of xenon 5p at both distances. At R_e, this MO has smaller coefficients on the 2p orbitals of atoms B(2), B(4), B(8), and B(10) and the 1s orbitals of the bridging hydrogens. The total populations for the $11a_1$ and $10a_1$ (at R_e) are approximately independent of distance. The same behavior holds for the $6b_2$ (-0.490 E_h) and $7b_2$ (-0.476 E_h) MOs, but with less change for the individual MOs. Table 9 shows the gross atomic populations for all atoms for $B_{10}H_{14}Xe$ at equilibrium and at $R = 100$ b. The total electronic charge of Xe suggests no significant electron charge transfer from this atom. The polar decaborane induces a dipole moment in the Xe atom, which interacts with the permanent dipole moment of $B_{10}H_{14}$.

3.5. Single-Reference SO−CISD Results for $B_{10}H_{14}Xe$. Single-reference SO−CISD calculations were carried out on the ground state of $B_{10}H_{14}Xe$, requiring a total of ca. 4.2×10^7 CSFs. The reference configuration of $B_{10}H_{14}Xe$ at R_e has a CI coefficient close to 0.88. The three characteristic doubly excited configurations of $B_{10}H_{14}$ appear in the same manner as before. Most of the double excitations come from $6b_1$ (-0.476 E_h) and $7b_2$ (-0.476 E_h). Both of these MOs have mostly Xe 5p atomic character. Excitation from orbitals with Xe 4d character is noticeable but not very significant. The virtual MOs that contribute the most to the correlation energy have as contributing AOs the 2s on the B(2), B(4), and B(8) atoms, the 2p on B(2), B(4), B(8), and B(10), and the 4d type on Xe to some extent. At $R = 100$ b, some single excitations with approximately the same magnitude CI coefficients appear. Some of these are for CSFs with different spatial symmetry than the reference CSF and are due to spin−orbit mixing,[40] commonly observed for both xenon and iodide.

The SO−CISD method gives the binding energy of decaborane with xenon as 0.96 kcal/mol (see Table 8). Whereas at the SCF level of theory $B_{10}H_{14}Xe$ appears to be slightly unbound, the singles and doubles correlation treatment of the system shows that it is in fact very weakly bound.

TABLE 12: Wave Function Based Results for $B_{10}H_{14}Xe$[a]

method	BE, ΔE^{CP}	BE, ΔE^{noCP}
CCSD(T)	1.09	1.94
CCSD	0.91	1.70
MP2	1.51	2.33
SO−CISD		0.96
SCF		−0.23

[a] The binding energy (BE) is in kcal/mol and CP denotes counterpoise procedure.

TABLE 13: DFT and SO-DFT Results for $B_{10}H_{14}Xe$[a]

functionals	BE, ΔE^{CP}	BE, ΔE^{noCP}
B3LYP	−0.37	−0.11
B3PW91	−0.57	−0.37
PW91PW91	0.74	1.02
PBE0	0.41	0.62
PW91PW91(SODFT)	0.75	

[a] The binding energy (BE) is in kcal/mol and CP denotes counterpoise procedure.

3.6. MP2, CCSD, CCSD(T), and DFT Results for $B_{10}H_{14}Xe$. Tables 12 and 13 summarize our wave function based and DFT results, respectively, for $B_{10}H_{14}Xe$. Table 12 indicates that the inclusion of triple excitations in CCSD(T) has a larger effect on the binding energy when the system is bound mostly by dispersion forces. Since the dispersion interaction is due to electron correlation, triple excitations contribute significantly in addition to the double excitations.[41−45] Along the same lines, methods such as MP2 (and MP3) are less suitable for the quantitative description of dispersion effects. Table 13 shows that the B3LYP and B3PW91 functionals completely fail to describe the binding of $B_{10}H_{14}Xe$, while the PW91PW91 and PBE0 functionals underestimate the binding energy, with the latter deviating significantly from our CCSD(T) result. The spin−orbit corrections do not contribute much to the binding energy within the PW91PW91 framework.

4. Discussion

The results in Tables 10−13 indicate several things. Some wave function based and DFT methods for $B_{10}H_{14}I^-$ give reliable binding energies, but at the level of chemical accuracy, small discrepancies appear. The energy values are also strongly affected by the BSSE, which corrects overestimates of the binding energy. Since the CCSD(T) results have the most accurate correlation treatment, we compare the results of other calculations to them, in the absence of any relevant experimental information. The CP binding energy was calculated to be 19.84 kcal/mol, whereas the corresponding energy without the BSSE correction was calculated to be 25.30 kcal/mol. Hence, the error in the calculation due to BSSE is 5.46 kcal/mol, approximately the same size as the correlation energy contribution to the binding. The CCSD method gives a value of 18.95 kcal/mol and, by comparison with the corresponding CCSD(T) result, gives 0.89 kcal/mol as the contribution of the connected triple excitations to the binding energy. An alternative highly correlated wave function based method is SO−CISD, which gave a value of 19.23 kcal/mol, quite close to the CCSD(T) value. Finally, MP2 did a good job in giving a relatively close (20.75 kcal/mol) value to the CCSD(T) binding energy for $B_{10}H_{14}I^-$, overshooting it by 0.91 kcal/mol. The BSSE values for CCSD-(T), CCSD, and MP2 were approximately 5 kcal/mol, showing the need for their inclusion. In terms of decreasing quality of

calculated binding energy, the DFT functionals used were ordered as B3PW91, PBE0, PW91PW91, and B3LYP (Table 11). It is also notable that the BSSE does not play an important role in the DFT results. These calculations suggest that the electrostatic nature of the binding energy can be adequately described by DFT methods.

$B_{10}H_{14}Xe$ is stabilized by weaker intermolecular forces (dispersion and dipole−induced-dipole). As a correlation effect, dispersion interactions are one of the most difficult interactions to calculate and cannot be described at the Hartree−Fock level. The accurate calculation of dispersion interactions necessitates the use of highly correlated wave function based techniques. Our CCSD(T) result of 1.09 kcal/mol shows that $B_{10}H_{14}Xe$ is indeed a very weakly bound system. The corresponding CCSD result (0.91 kcal/mol) shows that the triple excitations contribute 0.18 kcal/mol. The SO−CISD method does a good job in giving a binding energy of 0.96 kcal/mol. The MP2 method, as with $B_{10}H_{14}I^-$, provides an overly large value of 1.51 kcal/mol. As expected, the Hartree−Fock result gives no binding. In $B_{10}H_{14}Xe$, the contamination due to BSSE is considerably higher than in $B_{10}H_{14}I^-$; the values for the CCSD(T), CCSD, and MP2 methods are 0.85, 0.79, and 0.82 kcal/mol, respectively (compared to the CP-corrected binding energy of 1.09 kcal/mol).

One goal of the present study is to test a number of (computationally cheaper) DFT methods and determine if any of them can be used to describe dispersion forces sufficiently well for practical studies of similar systems. Approximate DFT functionals do not necessarily include all correlation effects well enough to describe dispersion interactions.[46−53] For the weakly bound van der Waals complex of $B_{10}H_{14}Xe$, the PW91PW91 and PBE0 functionals generate values for the interaction energy that are comparable with higher-level wave function based methodologies. The PW91 functional is the most reliable for treating benzene van der Waals complexes.[54,55] The PW91 exchange functional is best used with the corresponding correlation functional (PW91PW91), since in this case, the errors in exchange and correlation contributions tend to cancel.[35] The similarity of the CP binding energies between the CCSD(T) method (1.09 kcal/mol) and PW91PW91 method (0.74 kcal/mol) is consistent with this. The PBE0 functional (the PBE exchange functional with the PBE correlation functional) has previously been found to give a good description of noble gas dimers,[53] but the PW91 and PBE0 functionals also give binding with the correlation potential excluded, indicating that the exchange functionals contain some correlation. The calculation of the CP binding energy of $B_{10}H_{14}Xe$ with the PBE0 functional predicts a weakly bound complex (with a CP binding energy of 0.41 kcal/mol) but is not accurate. The B3LYP and B3PW91 DFT methods, as expected, give unbound complexes.[46,47,49,53] Their CP binding energies are computed to be −0.37 kcal/mol and −0.57 kcal/mol, respectively. Last, it needs to be emphasized that the BSSE errors for the most reliable functionals PW91PW91 (0.28 kcal/mol) and PBE0 (0.21 kcal/mol) are relatively large, however, less than that found for the wave function based methods.

5. Conclusions

The substantially larger binding energy for the I^- complex compared to the Xe complex shows that the charge (and polarizability) of I^- play the largest role in the interaction with $B_{10}H_{14}$. Significant improvement was made on the RECP basis sets of I and Xe, and care was taken for the use of balanced basis sets. Although early reports were justifiably pessimistic about the ability of DFT to describe dispersion interactions, the present study has found that DFT methods with certain exchange-correlation functionals do describe this interaction. In particular, the PW91PW91 and PBE0 functionals are the better choices for studying weak-interaction systems. Other functionals also gave realistic descriptions of the interaction energy in $B_{10}H_{14}I^-$. If one takes the high-level wave function based estimates as a reliable reference, we can conclude that selected DFT methods can be efficient alternatives when dealing with very large systems. It has also been found that the CP for BSSE is necessary when comparing different computational approaches.

Acknowledgment. We thank S. Brozell, R. Shepard, V.-A. Glezakou, R. Tyagi, S. G. Shore, P. A. Christiansen, T. Mueller, S. S. Xantheas, and Z. Zhang for useful discussions and help with the codes. We acknowledge the use of the computational facilities at the Ohio Supercomputer Center and the help provided by the High Performance Computational Chemistry Group, *NWChem, A Computational Chemistry Package for Parallel Computers*, version 4.1 (2002), Pacific Northwest National Laboratory, Richland, WA. This work was supported by the U. S. Department of Energy, Office of Basic Energy Sciences, grant ER15136.

References and Notes

(1) Wermer, J. R.; Hollander, O.; Huffman, J. C.; Krause Bauer, J. A.; Dou, D.; Hsu, L.-Y.; Leussing, D. L.; Shore, S. G. *Inorg. Chem.* **1995**, *34*, 3065 and references therein.

(2) Liu, B.; McLean, A. D. *J. Chem. Phys.* **1973**, *59*, 4557.

(3) van Duijneveldt, F. B.; van Duijneveldt-van de Rijdt, J. G. C. M.; van Lenthe, J. H. *Chem. Rev.* **1994**, *94*, 1873.

(4) Boys, S. F.; Bernardi, F. *Mol. Phys.* **1970**, *19*, 553.

(5) van Mourik, T.; Wilson, A. K.; Peterson, K. A.; Woon, D. E.; Dunning, T. H. *Adv. Quantum Chem.* **1998**, *31*, 105−132.

(6) Xantheas, S. S *J. Chem. Phys.* **1996**, *104*, 8821.

(7) See www.clarkson.edu/~pac/reps.html for complete references and a library of potentials.

(8) Pacios, L. F.; Christiansen, P. A. *J. Chem. Phys.* **1985**, *82*, 2664.

(9) Hurley, M. M.; Pacios, L. F.; Christiansen, P. A.; Ross, R. B.; Ermler, W. C. *J. Chem. Phys.* **1986**, *84*, 6840.

(10) LaJohn, L. A.; Christiansen, P. A.; Ross, R. B.; Atashroo, T.; Ermler, W. C. *J. Chem. Phys.* **1987**, *87*, 2812.

(11) Ross, R. B.; Powers, J. M.; Atashroo, T.; Ermler, W. C.; LaJohn, L. A.; Christiansen, P. A. *J. Chem. Phys.* **1990**, *93*, 6654.

(12) Ermler, W. C.; Ross, R. B.; Christiansen, P. A. *Int. J. Quantum Chem.* **1991**, *40*, 829.

(13) Lee, Y. S.; Ermler, W. C.; Pitzer, K. S. *J. Chem. Phys.* **1977**, *67*, 5861.

(14) Christiansen, P. A.; Lee, Y. S.; Pitzer, K. S. *J. Chem. Phys.* **1979**, *71*, 4445.

(15) Ross, R. B.; Ermler, W. C.; Christiansen, P. A. *J. Chem. Phys.* **1986**, *84*, 3297.

(16) Dunning, T. H. *J. Chem. Phys.* **1989**, *90*, 1007.

(17) Christiansen, P. A. *J. Chem. Phys.* **2000**, *112*, 10070.

(18) Blaudeau, J.-P.; Brozell, S. R.; Matsika, S.; Zhang, Z.; Pitzer, R. M. *Int. J. Quantum Chem.* **2000**, *77*, 516.

(19) Wallace, N. M.; Blaudeau, J.-P.; Pitzer, R. M. *Int. J. Quantum Chem.* **1991**, *40*, 78.

(20) Martin, J. M. L.; Sundermann, A. *J. Chem. Phys.* **2001**, *114*, 3408.

(21) The basis sets where we took the f exponents are located in http://theochem.weizmann.ac.il/web/papers/SDB-cc.html.

(22) Peterson, K. A.; Figgen, D.; Goll, E.; Stoll, H.; Dolg, M. *J. Chem. Phys.* **2003**, *119*, 11113.

(23) See http://www.emsl.pnl.gov:2080/forms/basisform.html.

(24) COLUMBUS programs are described at http://www.itc.univie.ac.at/~hans/Columbus/Columbus.html.

(25) Harrison, R. J.; Nichols, J. A.; Straatsma, T. P.; Dupuis, M.; Bylaska, E. J.; Fann, G. I.; Windus, T. L.; Apra, E.; de Jong, W.; Hirata, S.; Hackler, M. T.; Anchell, J.; Bernholdt, D.; Borowski, P.; Clark, T.; Clerc, D.; Dachsel, H.; Deegan, M.; Dyall, K.; Elwood, D.; Fruchtl, H.; Glendening, E.; Gutowski, M.; Hirao, K.; Hess, A.; Jaffe, J.; Johnson, B.; Ju, J.; Kendall, R.; Kobayashi, R.; Kutteh, R.; Lin, Z.; Littlefield, R.; Long, X.; Meng, B.; Nakajima, T.; Nieplocha, J.; Niu, S.; Rosing, M.; Sandrone, G.; Stave, M.; Taylor, H.; Thomas, G.; van Lenthe, J.; Wolinski, K.; Wong,

A.; Zhang, Z. *NWChem, A Computational Chemistry Package for Parallel Computers*, version 4.1; Pacific Northwest National Laboratory: Richland, WA, 2002.
(26) Noga, J.; Bartlett, R. J. *J. Chem. Phys.* **1987**, *86*, 7041.
(27) Noga, J.; Bartlett, R. J. *J. Chem. Phys.* **1988**, *89*, 3401.
(28) Kucharski, S. A.; Bartlett, R. J. *J. Chem. Phys.* **1992**, *97*, 4282.
(29) Raghavachari, K.; Trucks, G. W.; Pople, J. A.; Head-Gordon, M. *Chem. Phys. Lett.* **1989**, *157*, 479.
(30) Raghavachari, K.; Pople, J. A.; Replogle, E. S.; Head-Gordon, M. *J. Phys. Chem.* **1990**, *94*, 5579.
(31) Hohenberg, P.; Kohn, W. *Phys. Rev. B: Condens. Matter* **1964**, *136*, 864.
(32) Kohn, W.; Sham, L. J. *Phys. Rev. A: At., Mol., Opt. Phys.* **1965**, *140*, 1131.
(33) Becke, A. D. *J. Chem. Phys.* **1993**, *98*, 5648.
(34) Lee, C.; Yang, W.; Parr, R. G. *Phys. Rev. B: Condens. Matter* **1988**, *37*, 785.
(35) Perdew, J. P.; Chevary, J. A.; Vosko, S. H.; Jackson, K. A.; Pederson, M. R.; Singh, D. J.; Fiolhais, C. *Phys. Rev. B: Condens. Matter* **1992**, *46*, 6671.
(36) Adamo, C.; Barone, V. *J. Chem. Phys.* **1998**, *110*, 6158.
(37) Van der Maas Redy, J.; Lipscomb, W. N. *J. Am. Chem. Soc.* **1959**, *81*, 754.
(38) Sands, D.; Zalkin, A. *Acta Crystallogr.* **1962**, *15*, 410.
(39) Dunning, T. H. *J. Phys. Chem. A* **2000**, *104*, 9062.
(40) Yabushita, S.; Zhang, Z.; Pitzer, R. M. *J. Phys. Chem. A* **1999**, *103*, 5791.
(41) Briggs, M. P.; Murrell, J. N.; Stamper, J. G. *Mol. Phys.* **1969**, *17*, 381.
(42) Riemenschneider, B. M.; Kestner, N. R. *Chem. Phys.* **1974**, *3*, 193.
(43) Maeder, F.; Kutzelnigg, W. *Chem. Phys. Lett.* **1976**, *37*, 285.
(44) Kutzelnigg, W. *Faraday Discuss. Chem. Soc.* **1977**, *62*, 185.
(45) Meyer, W.; Hariharan, P. C.; Kutzelnigg, W. *J. Chem. Phys.* **1980**, *73*, 1880.
(46) Kristyan, S.; Pulay, P. *Chem. Phys. Lett.* **1994**, *229*, 175.
(47) Hobza, P.; Šponer, J.; Reschel, T. *J. Comput. Chem.* **1995**, *16*, 1315.
(48) Šponer, J.; Leszczynski, J.; Hobza, P. *J. Biomol. Str. Dyn.* **1996**, *14*, 117−135.
(49) Rappé, A. K.; Bernstein, E. R. *J. Phys. Chem. A* **2000**, *104*, 6117.
(50) Chalashiński, G.; Szczęśniak, M. M. *Chem. Rev.* **2000**, *100*, 4227−4252.
(51) Meier, R. J. *Faraday Discuss.* **2003**, *124*, 405.
(52) Görling, A. *J. Chem. Phys.* **2005**, *123*, 62203.
(53) Xu, X.; Zhang, Q.; Muller, R. P.; Goddard, W. A. *J. Chem. Phys.* **2005**, *122*, 14105.
(54) Wesolowski, T. A.; Parisel, O.; Ellinger, Y.; Weber, J. *J. Phys. Chem. A* **1997**, *101*, 7818.
(55) Wesolowski, T. A.; Ellinger, Y.; Weber, J. *J. Chem. Phys.* **1998**, *108*, 6078.